Ab Initio and Density Functional Investigation of Reactions of NO with XCO (X = H, F, Cl)

Sudhir A. Kulkarni*,†,‡ and Nobuaki Koga‡

Department of Chemistry, University of Pune, Pune 411 007, India, and School of Informatics and Sciences, Nagoya University, Nagoya 464-01, Japan

Received: August 4, 1997; In Final Form: December 19, 1997

Ab initio as well as density functional methods are used to investigate various reaction paths for XCO + NO (X = H, F, Cl) with a special focus on the reaction path through the collisional complex CX(O)NO, which is experimentally proposed for X = H and F. It is revealed that the dissociation channels of CH(O)NO to HNO + CO and CF(O)NO to FNO + CO have a higher barrier, while the CCl(O)NO has a dissociation barrier lower than that of the redissociation to reactants. It is expected that this channel should be the major one for the disappearance of CCl(O)NO. To gauge the relative importance of various channels of CX(O)NO disappearance, high-pressure RRKM rate constants are obtained. These results suggest the necessity of reinvestigation of a model based on experiments for the HCO + NO reaction. For the reactions of FCO and ClCO with NO, the MP2 and B3LYP stationary point structures and relative energies are in reasonable agreement with each other, whereas for the HCO + NO reaction, the MP2 level PES is markedly different from the QCISD and B3LYP counterparts.

I. Introduction

The formyl (HCO), fluoroformyl (FCO), and chloroformyl (ClCO) radicals are the reactive intermediates formed during oxidation of hydrocarbons and halogenated hydrocarbons. Detailed understanding of the reactions of these radicals with O_2 and NO is extremely crucial for the knowledge of their effects on the environment. Several experiments investigating the kinetics of these important reactions have been carried out[1−5] for this purpose.

For the study of kinetics of the reaction of HCO with NO, two possible pathways were considered[1,2] earlier:

$$\mathrm{HCO + NO \rightarrow HNO + CO} \quad (1)$$

$$\mathrm{HCO + NO \rightleftharpoons CH(O)NO \rightarrow HNO + CO} \quad (2)$$

However, the inverse kinetic isotope effect observed for this reaction[2] rules out the direct hydrogen abstraction mechanism (1). The other pathway (2) proposed by Langford and Moore (LM)[2] assumes the formation and decomposition of an adduct or a complex, such as CH(O)NO. From pressure independence of the reaction rates, it was inferred that the fast dissociation of this complex takes place to yield either the products or the reactants. This model was further supported by semiquantitative RRKM calculations[2] and also by Tsang et al.[3] in a recent study. However, the existence of some other competitive channels such as isomerization of CH(O)NO cannot be ruled out. One of the aims of the present study is to investigate such pathways along with the one proposed by LM.

Experimental studies of the kinetics of the reaction of FCO at room temperature with variable pressures have been reported.[4,5] The strong pressure dependence of the rate constants essentially indicates an intermediate stable complex, CF(O)NO. Although an intermediate complex is assumed to be formed in the reactions of HCO and FCO with NO, both these reactions differ in their pressure dependence. Although CH(O)NO was proposed[2] to dissociate to the reactants or products before getting stabilized, considerable stabilization has been indicated for the species CF(O)NO.[5]

Similar reactions of XCO + O_2 have been investigated theoretically as well as experimentally.[2−4,6−8] Theoretical investigation of the reaction of HCO + O_2 over a wide range of temperatures and pressures has recently been reported by Hsu et al.[6] Their calculations support the model proposed by LM.[2] The activation barrier for the dissociation of $CH(O)O_2$ to HO_2 + CO is lower than that for redissociation to the reactants. The RRKM rate constant of about 10^{-11} $cm^3/(mol\ s)$ over a wide temperature range indicates that it is the major channel. The rate constants for the isomerization of $CH(O)O_2$ are temperature-dependent; however, at the room temperature, the contribution of this reaction to the total raction rate is not significant. Further, the calculated total reaction rates showed pressure independence, in agreement with the experimental results. An ab initio study of the reaction of FCO with O_2 has shown that the formation of $FC(O)O_2$ is an exothermic and barrierless process.[7] The extraction of fluorine from FCO by O_2 to yield FO_2 and CO is an endothermic process without a barrier. Theoretical estimates of the heats of reaction[8] of ClCO with O_2 have been reported as well.

In view of the above experimental and theoretical reports, we have taken up an ab initio study of the reactions of NO with XCO for X = H, F, and Cl. The structures and relative energies of the stationary points are calculated to investigate the reaction mechanism. Although the mechanistic path passing through a collisional complex has been experimentally proposed, the present work takes into account other reaction channels for X = H. However, for X = F and Cl we focused on the reaction mechanism through the complex CX(O)NO and compared its stability among H, F, and Cl on the basis of the barriers to dissociation. Further, the model by LM[2] is critically appraised

* To whom correspondence should be addressed. E-mail: sakul@chem.unipune.ernet.in.
† University of Pune.
‡ Nagoya University.

S1089-5639(97)02541-3 CCC: $15.00
Published on Web 06/17/1998

in light of the ab initio results and the rate constants calculated using statistical methods.

II. Computational Methods

The ab initio calculations at the unrestricted second-order Møller−Plesset perturbation (MP2) level with the 6-31+G(d) basis set (denoted henceforth as UMP2/6-31+G(d)) are performed using Gaussian 94[9] to locate the stationary points on the singlet potential energy surface (PES) of XCO + NO (X = H, F, Cl). The unrestricted wave functions are employed in the present study, since the restricted wave functions for some of the stationary points are found to be unstable.

More reliable energies are evaluated by the projected full fourth-order Møller−Plesset perturbation theory (PMP4(SDTQ)) and unrestricted quadratic configuration interaction method including singles, doubles, and triples (QCISD(T)) with the same basis set. Further, G2(MP2) energies[10] are obtained for some stationary points. In addition, these reactions are studied within the realm of the density functional theory (DFT) using an unrestricted Becke three-parameter hybrid method with the Lee, Yang, and Parr correlation functional with the 6-311G(d,p) basis set (denoted as B3LYP/6-311G(d,p)), and the results thus obtained are compared with the UMP2 level structures and energetics. Single-point energy calculations at the B3LYP optimized geometries are carried out using the PMP4(SDTQ) method and the unrestricted coupled cluster method including singles, doubles, and triples (CCSD(T)) with the 6-311G(d,p) basis set. For the HCO + NO reaction, some stationary points are located by the quadratic configuration interaction including singles and doubles with 6-31G(d) basis set (denoted as QCISD/6-31G(d)) as well. The vibrational frequencies of all the stationary points are obtained at both the MP2 and B3LYP levels and later used in the RRKM calculations without scaling. The reaction pathways are followed by the intrinsic reaction coordinate (IRC) method. We have used notations such as CCSD(T)//B3LYP to indicate a CCSD(T) calculation performed with the B3LYP geometry in the following sections.

III. Results and Discussion

The various reaction pathways for XCO + NO reaction considered here are

$$\mathrm{XCO + NO} \xrightarrow{a} \mathrm{XNO + CO}$$

$$\mathrm{XCO + NO} \underset{c}{\overset{b}{\rightleftharpoons}} \mathrm{CX(O)NO} \xrightarrow{d} \mathrm{XNO + CO}$$

$$\xrightarrow{e} \text{isomerization} \rightarrow \text{product}$$

$$\mathrm{XCO + NO} \xrightarrow{f} \text{complex formation} \rightarrow \mathrm{XNO + CO}$$

The relative energies calculated at various levels for the UMP2/6-31+G(d) and B3LYP/6-311G(d,p) optimized structures are reported in Tables 1−3. Note that NO has a singly occupied π^* orbital in the ground state ($^2\Pi$), and XCO is a σ radical ($^2A'$).

III.1. Reaction of HCO + NO. The structures of stationary points on the UMP2/6-31+G(d) PES of HCO + NO reaction are portrayed in Figure 1, and the corresponding energy profiles for possible reaction pathways calculated for those geometries are depicted in Figure 2. As shown in Figure 2, we have considered three reaction channels for the formation of HNO + CO from HCO + NO: (1) a direct hydrogen abstraction path through TSM2, (2) a path that includes the formation and dissociation of CH(O)NO via TSM1, and (3) a channel forming the HCO···ON complex and passing through TSM3. The transition states (TSs) determined at the UMP2 level are designated as TSM in this section, whereas those at the B3LYP level are designated as TS.

The direct hydrogen abstraction path has a barrier of 2.35 kcal/mol at the PMP2 level to form HNO + CO. At TSM2, an odd electron occupying the in-plane π^* orbital of NO abstracts the hydrogen atom to form HNO and CO. The single-point energy calculations for TSM2 at the PMP4 and QCISD(T) levels indicated that this path is a downhill one (as shown in Figure 2). The estimates of the reaction rate on this path using general transition-state theory (TST) are obtained from

TABLE 1: Relative Energies Including ZPE in kcal/mol and $\langle S^2 \rangle$ before Projection of Reactants, Products, Intermediates, and Transition States of HCO + NO Reaction

(A) At UMP2/6-31+G(d) Geometry[a]

species	$\langle S^2 \rangle$	PMP2	PMP4	QCISD(T)	G2(MP2)[b]
HCO + NO	0.77, 0.78	0.00	0.00	0.00	0.00
HNO + CO	0.0, 0.0	−32.50	−34.48	−35.47	−34.48
CH(O)NO	0.48	−28.15	−27.90	−29.61	−29.16
HCO···NO	0.97	15.70	11.32	8.16	8.23
TSM1	0.0	16.50	12.49	19.66	12.74
TSM2	0.51	2.35	−13.93	−20.60	−0.12
TSM3	0.78	15.20	10.80	8.00	
TSM4	0.80	−5.37	−7.66		

(B) At B3LYP/6-311G(d,p) Geometry[c]

species	$\langle S^2 \rangle$	B3LYP	PMP2	PMP4	CCSD(T)
HCO + NO	0.75, 0.75	0.00	0.00	0.00	0.00
HNO + CO	0.0, 0.0	−25.36	−29.09	−30.96	−32.81
NOH + CO	2.0, 0.0	−6.34	−5.34	−7.32	−10.34
CH(O)NO	0.43	−24.67	−22.03	−21.31	−23.54
HNOCO	0.0	−7.83	3.49	4.88	3.89
HONCO	0.0	−45.29	−40.27	−37.37	−37.97
TS1	0.0	12.43	13.94	7.87	12.55
TS2	0.0	14.11	20.70	19.11	23.17
TS3	0.32	−6.77	0.90	−1.21	2.48
TS4	0.0	14.95	27.15	27.68	26.46
TS5	0.0	15.49	22.17	17.05	13.95

[a] The total energies of HCO + NO are −243.115 87, −243.158 92, −243.150 89, and −243.432 19 au at PMP2, PMP4, QCISD(T), and G2(MP2) levels, respectively. [b] See ref 10 for the method. [c] The total energies of HCO + NO are −243.813 29, −243.219 51, −243.255 94 and −243.255 64 au at B3LYP, PMP2, PMP4, and CCSD(T) levels, respectively.

TABLE 2: Relative Energies Including ZPE in kcal/mol and $\langle S^2 \rangle$ before Projection of Reactants, Products, Intermediates, and Transition States of FCO + NO Reaction

(A) At UMP2/6-31+G(d) Geometry[a]

species	$\langle S^2 \rangle$	PMP2	PMP4	QCISD(T)
FCO + NO	0.78, 0.78	0.00	0.00	0.00
FNO + CO	0.0, 0.0	−30.91	−36.17	−31.87
CF(O)NO	0.43	−30.35	−30.42	−31.72
TS1	0.0	3.17	−3.58	6.00

(B) At B3LYP/6-311G(d,p) Geometry[b]

species	$\langle S^2 \rangle$	B3LYP	PMP2	PMP4	CCSD(T)
FCO + NO	0.75, 0.75	0.00	0.00	0.00	0.00
FNO + CO	0.0, 0.0	−20.86	−22.34	−26.96	−24.47
CF(O)NO	0.28	−27.20	−25.33	−24.97	−26.62
TS1	0.0	6.87	13.00	4.87	14.75

[a] The total energies of FCO + NO are −342.155 84, −342.201 71, and −342.191 53 au at PMP2, PMP4, and QCISD(T) levels, respectively. [b] The total energies of FCO + NO are −343.088 28, −342.305 16, −342.353 04, and −342.340 35 au at B3LYP, PMP2, PMP4, and CCSD(T) levels, respectively.

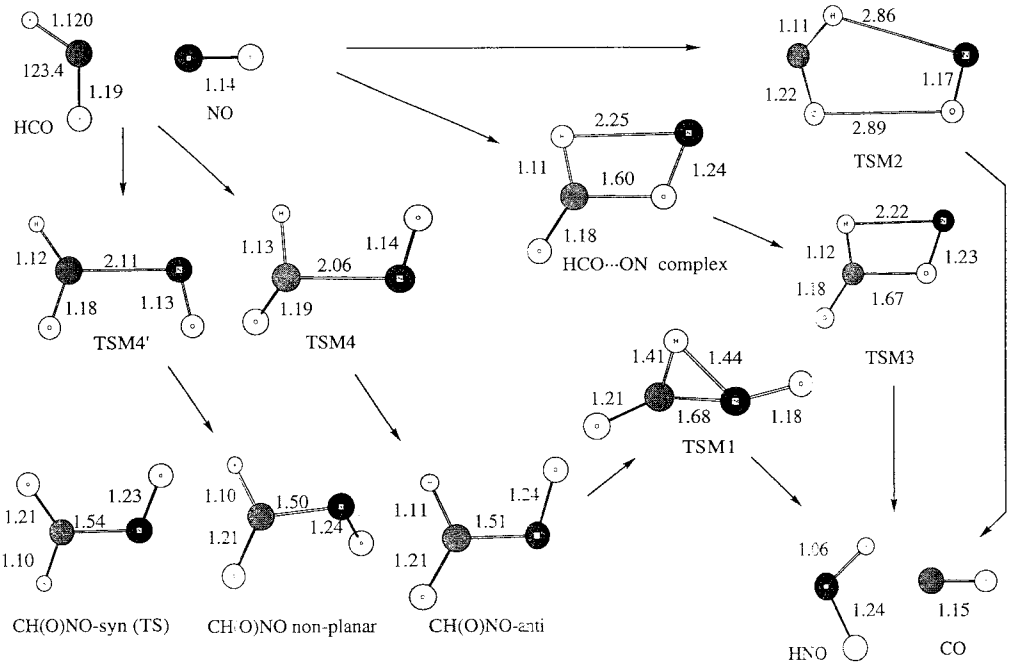

Figure 1. Optimized structures of stationary points on the potential energy surface of HCO + NO at the UMP2/6-31+G(d) level. All bond lengths are in angstroms and angles in degrees.

TABLE 3: Relative Energies and (ZPE) in kcal/mol and $\langle S^2 \rangle$ before Projection of Reactants, Products, Intermediates, and Transition States of ClCO + NO Reaction

(A) At UMP2/6-31+G(d) Geometry[a]

species	$\langle S^2 \rangle$	PMP2	PMP4	QCISD(T)
ClCO + NO	0.78, 0.78	0.00	0.00	0.00
ClNO + CO	0.0, 0.0	−30.91	−35.40	−34.49
CCl(O)NO	0.0	−26.62	−26.48	−27.35
TS1	0.0	−5.13	−11.50	−2.87

(B) At B3LYP/6-311G(d,p) Geometry[b]

species	$\langle S^2 \rangle$	B3LYP	PMP2	PMP4	CCSD(T)
ClCO + NO	0.76, 0.75	0.00	0.00	0.00	0.00
ClNO + CO	0.0, 0.0	−28.62	−28.53	−32.02	−30.28
CCl(O)NO	0.0	−20.66	−19.19	−18.95	−20.32
TS1	0.0	−6.10	−1.00	−5.38	1.09

[a] The total energies of ClCO + NO are −702.160 79, −702.217 09, and −702.207 55 au at PMP2, PMP4, and QCISD(T) levels, respectively. [b] The total energies of ClCO + NO are −703.452 48, −702.288 11, −702.347 33, and −702.334 48 au at B3LYP, PMP2, PMP4, and CCSD(T) levels, respectively.

$k(T, s) = (\alpha k_B T/h) \exp[-\Delta G(T, s)/(k_B T)]$. Here, s is the reaction coordinate, α denotes the statistical factor, k_B is the Boltzmann constant, h is Planck's constant, and ΔG is the standard free energy of activation. We have used $s = 0.0$, which leads to the rate constant using simple TST. Assuming that this channel is barrierless, the rate constant would turn out to be 1.1×10^{-17} cm^3 molecule^{-1} s^{-1} at 298 K, indicating that this channel does not contribute significantly to the total reaction rate.

The second possible path involves the formation and dissociation of CH(O)NO. This complex exhibits a minimum for a planar structure with oxygen atoms being anti around C−N bond as well as for a nonplanar structure. The latter turns out to be 2.7 kcal/mol less stable than the former. On the other hand, a planar structure with the oxygen atoms disposed syn around the C−N bond has one imaginary frequency and is 0.4 kcal/mol higher in energy compared with the nonplanar minimum. Thus, it is the TS for rotation around the C−N bond between the two nonplanar structures. Note that the RMP2

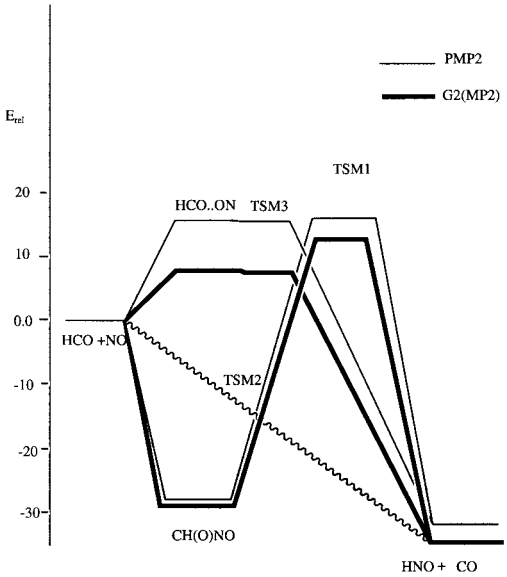

Figure 2. Relative energies including zero-point energy correction (ZPE) of stationary points on the potential energy surface of HCO + NO at the UMP2/6-31+G(d) level.

structure of CH(O)NO shows no significant difference in the geometrical parameters, and it is only 0.05 kcal/mol higher in energy compared with the corresponding UMP2 structure. This indicates that the effect of spin contamination (of $\langle S^2 \rangle = 0.48$) on the structure is negligible in this case.

Since the formation of CH(O)NO involves the coupling of radicals, the reaction is expected to be exothermic and barrierless. The formation of the planar anti CH(O)NO is an exothermic reaction with a barrier of 10.55 kcal/mol at the UMP2 level (cf. TSM4 in Figure 1). Upon inclusion of corrections to the spin contamination at the PMP2 and higher levels, the reaction becomes barrierless (cf. Table 1A). The higher $\langle S^2 \rangle$ for TSM4 in Table 1A suggests that the antibonding triplet contamination artificially destabilizes the structure. Yet another TS (TSM4′, shown in Figure 1) for CH(O)NO formation exists on the UMP2 level PES. Analogous to TSM4, the

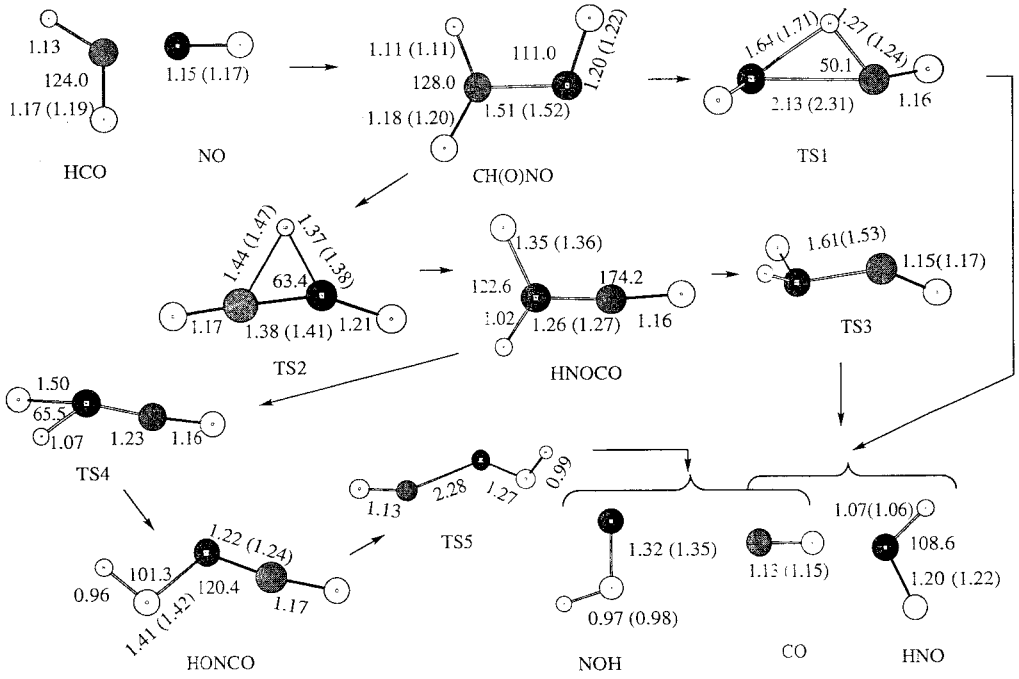

Figure 3. Optimized structures of stationary points on the potential energy surface of HCO + NO at the B3LYP/6-311G(d,p) level. The numbers in parentheses are structural parameters at the QCISD/6−31G(d) level. All bond lengths are in angstroms and angles in degrees.

formation of CH(O)NO through TSM4′ is barrierless at the PMP2 and higher level calculations. The IRC path from TSM4′ leads to the syn structure of CH(O)NO, which is also the TS for internal rotation as shown above. This indicates that before reaching syn CH(O)NO, there must be a point on the PES where the reaction coordinate bifurcates toward the two enantiomeric structures of the nonplanar CH(O)NO.

The decomposition pathway of CH(O)NO to form HNO + CO (step d, cf. Figure 2) has high barriers of 44.65, 40.39, and 49.27 kcal/mol at the PMP2, PMP4(SDTQ), and QCISD(T) levels, respectively. The G2(MP2) estimate for this barrier is 41.90 kcal/mol. The corresponding TS (TSM1 in Figure 1) has the hydrogen atom bridging the carbon and nitrogen atoms and migrating from the former to the latter along with the O−C−N−O dihedral angle of almost 180°. The high barrier for this decomposition reaction indicates that the reverse reaction to the reactants (step c) is favored over the decomposition of CH(O)NO giving HNO and CO. The path corresponding to the isomerization (step e) of CH(O)NO does not exist on the UMP2 level PES, although such a path exists on the Hartree−Fock level PES.

There exists yet another channel (step f) that contains the formation of a weak complex HCO···ON (cf. Figures 1 and 2). However, unlike the formation of a stable collisional complex CH(O)NO through TSM4, an intermediate structure in this channel is unstable at all levels of theory (cf. Table 1A). The in-plane π electrons of NO prefer to be at the oxygen rather than at the nitrogen because of the difference in electronegativity, and therefore, the structure of this complex is not favorable for any new bond formation and thus is less stable than the isolated reactants. From this complex, further reaction proceeds with the abstraction of hydrogen from HCO by NO to form HNO + CO, requiring a negligible barrier relative to the complex. Although the structure of the corresponding TS (TSM3 in Figure 1) is similar to the complex, it has hydrogen closer to the nitrogen and the C−ON bond is slightly elongated. At the PMP2 and higher levels, TSM3 is more stable than the HCO···ON complex. Thus, the complex or the TS between the reactants and the complex should be the least stable point on the reaction path, namely, the TS for this process. However, since no complex formation is favorable, the contribution of this reaction to the total reaction rate is not expected to be significant. Further, the inverse kinetic isotope effect is apparently not expected for this reaction; hence, we have not investigated this process further.

In summary, the MP2 calculations showed that among the reaction paths we have considered here, the path through CH(O)NO is the most plausible one. The possible reactions from CH(O)NO are either redissociation to the reactants or dissociation to the products. The latter process requires a larger activation energy and thus is less favorable.

On the basis of the results obtained with the MP2 structures, we studied this reaction by the B3LYP method to evaluate the performance of this density functional method usually considered to be reliable.[11] Various stationary structures obtained on the B3LYP/6-311G(d,p) PES are shown in Figure 3. The possible reaction channels and their relative energies are shown in Figure 4. Table 1B summarizes relative energies of all these structures at the B3LYP, PMP2, PMP4, and CCSD(T) levels calculated using the B3LYP structures. As depicted in Figure 4, the B3LYP/6-311G(d,p) paths are rather different from the UMP2/6-31+G(d) ones; the B3LYP level PES has both isomerization (step e) and dissociative (step d) paths from CH(O)NO leading to HNOCO and HNO + CO, respectively. There exist channels for the dissociation of HNOCO to HNO + CO and the isomerization of HNOCO to HONCO, which subsequently dissociates to NOH + CO also (cf. Figure 4).

For CH(O)NO, we took into account only the planar anti structure because it was shown in the above calculations to be the most stable. The CH(O)NO formation is a downhill process as inferred from the UMP2/6-31+G(d) calculations. The TS (TS1 in Figure 3) corresponding to the dissociative path has a longer C−N bond, and its hydrogen is closer to carbon compared to the corresponding TS (TSM1 in Figure 1) at the UMP2 level. The isomerization channel passing through TS2 has a compact structure **(**with a short C−N bond and an almost linear NCO group) and involves hydrogen migration toward the neighboring nitrogen (cf. structure TS2 in Figure 3). The

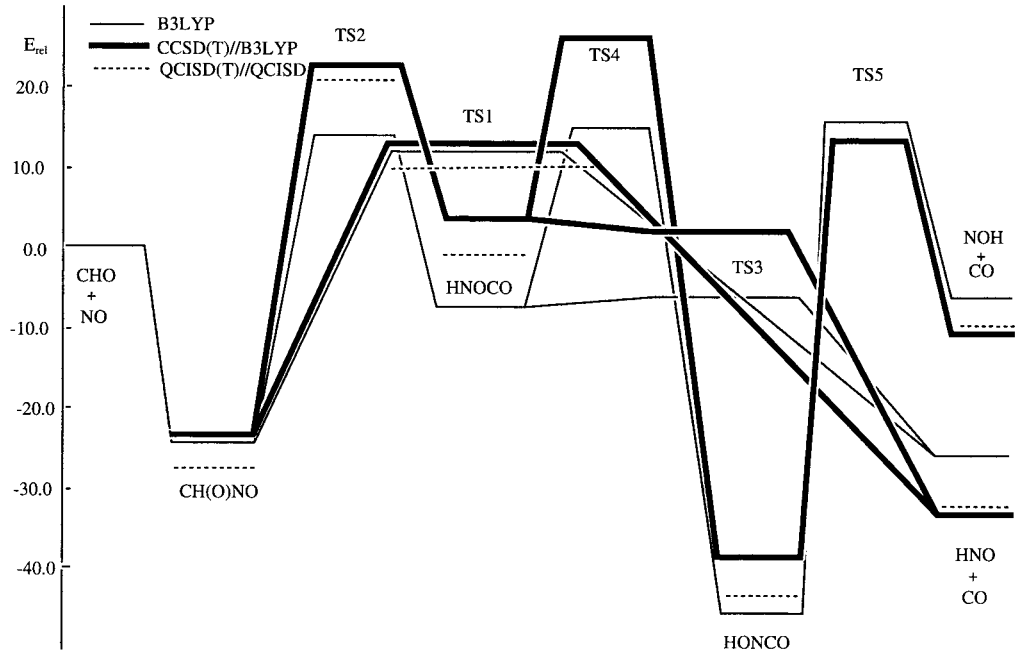

Figure 4. Relative energies including the ZPE of stationary points on the potential energy surface of HCO + NO at the B3LYP/6-311G(d,p) level. The dotted lines show QCISD(T)/6-311G(d,p)//QCISD/6-31G(d) energies without inclusion of ZPE for some structures.

B3LYP barriers for dissociation and isomerization are 37.10 and 38.78 kcal/mol, respectively, whereas they are 36.09 and 46.71 kcal/mol at the CCSD(T)//B3LYP level; the barrier for isomerization is higher than that for the dissociation reaction.

The isomerization product, HNOCO, exhibits a minimum on PES for both the planar and nonplanar structures with the latter being more stable by 1.2 kcal/mol than the former. However, the IRC calculations indicate that reaction channels pass through only the planar isomer shown in Figure 3. HNOCO dissociates into HNO + CO with a negligible barrier via TS3 wherein the HNO group is rotated and the C−N bond is stretched to 1.61 Å. The rotation makes the structure favorable for the interaction between the carbon lone pair of CO and the HNO π^* orbital, an interaction that stabilizes TS3. On the other hand, HNOCO can isomerize to HONCO via TS4 with a barrier of 22.78 kcal/mol at the B3LYP level. In TS4, the H−N−O angle is contracted from 123 to 65° and the N−O bond is stretched by 0.15 Å to facilitate hydrogen migration from nitrogen to oxygen. This isomerization is exothermic by −37.46 kcal/mol. HONCO is a planar molecule with an almost linear NCO group and an H−O−N−C dihedral angle of 180°. Another isomer of HONCO having an H−O−N−C dihedral angle of 0° is 6.1 kcal/mol higher in energy than the most stable one shown in Figure 3. This isomer has one imaginary frequency, implying that it is a TS for the internal rotation of the O−H bond around the O−N bond. HONCO dissociates to NOH + CO through TS5 in an endothermic reaction with a substantial barrier, viz. 60.78 and 51.92 kcal/mol at the B3LYP and CCSD(T)//B3LYP levels, respectively. In TS5, the C−N bond elongates by 1.06 Å compared to HONCO.

It is to be noted that there are several differences in the structures and relative energies of the B3LYP and MP2 levels. The TS for the dissociation of CH(O)NO has much shorter C−N bond at the MP2 level (TSM1) than at the B3LYP level (TS1). At the B3LYP level, there exist the TSs for isomerization of CH(O)NO to HNOCO (TS2) and that for dissociation from HNOCO to HNO + CO (TS3). The PMP2, PMP4, and CCSD(T) energy calculations at the B3LYP structures have shown that TS3 is more stable than HNOCO. This suggests that dissociation leading to HNO + CO is downhill and that HNOCO is not an equilibrium structure or has a transient existence, a result in consonance with those obtained by the MP2 geometry determinations. At the MP2 level, the B3LYP reaction path through TS2, HNOCO, and TS3 merges with that through TS1, as seen in the fact that the C−N distance in TSM1 is close to the average of those in TS1 and TS2.

To verify this conjecture, we have determined stationary points on these reaction channels at the QCISD/6-31G(d) level. Single-point energy calculations at the QCISD(T)/6-311G(d,p) level have been performed at the geometries thus optimized. The structural parameters of some stationary points are presented in Figure 3 and the relative energies in Figure 4. At the QCISD level, there exists a channel corresponding to the isomerization of CH(O)NO to HNOCO as shown in Figure 4. The QCISD TSs for the dissociation and isomerization of CH(O)NO have structures similar to the structures of B3LYP TSs, but the former TSs have a C−N bond longer by 0.2 and 0.03 Å, respectively, than that of the latter TSs. The barrier for dissociation of CH(O)NO is 37.6 kcal/mol, whereas the barrier to the isomerization is 48.8 kcal/mol. These barriers are comparable to those in the CCSD//B3LYP level calculations. Although the QCISD level barrier to the decomposition of HNOCO to HNO + CO through TS3 is 1.0 kcal/mol, the QCISD(T)//QCISD calculation indicates a downhill reaction path (−3.8 kcal/mol). This confirms the transient existence of HNOCO on this PES, similar to the MP2 results. TS2 is much less stable than TS1, and thus the path through TS2 can be reasonably neglected.

There are some other differences to be settled. The energy for the reaction HCO + NO leading to HNO + CO is found to be −34.5 to −35.5 kcal/mol at the PMP4//MP2, QCISD(T)//MP2, and G2(MP2)//MP2 levels and −25.4 kcal/mol at the B3LYP level, the difference being about 10 kcal/mol. The experimental estimate[2] of enthalpy change of the reaction is −30 kcal/mol at 298 K, indicating that the calculations using the MP2 structures overestimate the exothermicity, whereas those using the B3LYP ones underestimate it. The energy of the overall reaction is −32.6 kcal/mol at the QCISD(T)//QCISD level, which is close to that at the CCSD(T)//B3LYP level and

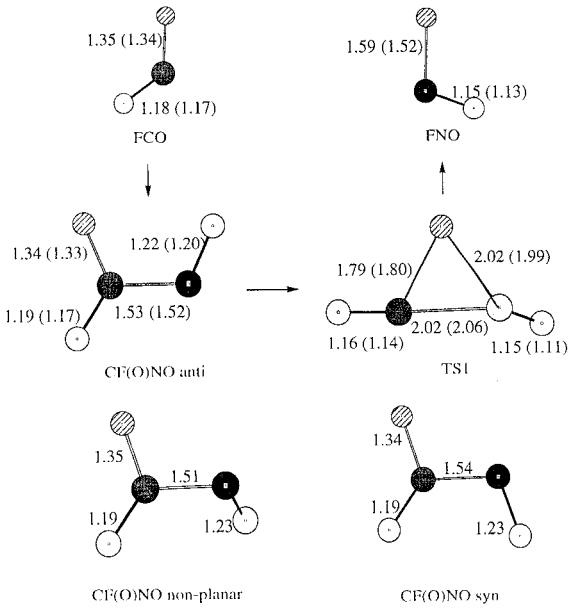

Figure 5. Optimized structures of stationary points on the potential energy surface of FCO + NO at the UMP2/6-31+G(d) level. The numbers in parentheses are structural parameters at the B3LYP/6-311G-(d) level. All bond lengths are in angstroms and angles in degrees.

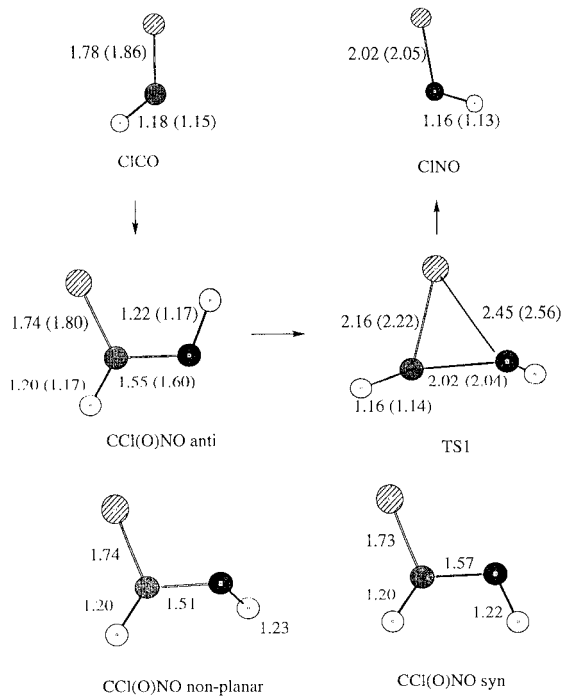

Figure 6. Optimized structures of stationary points on the potential energy surface of ClCO + NO at the UMP2/6-31+G(d) level. The numbers in parentheses are structural parameters at the B3LYP/6-311G-(d) level. All bond lengths are in angstroms and angles in degrees.

also to the experimental value. Further, the formation energy of CH(O)NO from HCO + NO obtained from various levels of theory at the MP2 structures is −28 to −30 kcal/mol, whereas by use of the B3LYP structure, it is −21 to −25 kcal/mol. At the QCISD(T)//QCISD level, it is −27.5 kcal/mol. The B3LYP binding energy is underestimated probably because of the too short CO and NO distances of CH(O)NO. Further, an extensive search of B3LYP level PES showed the absence of stationary structures on the reaction channel through step f.

Some general salient features of the reaction HCO + NO using experimental and theoretical methods are noteworthy. The model proposed by LM[2] based on RRKM calculations assumes that the energy of formation of CH(O)NO from the reactants is −32 kcal/mol and the corresponding barrier for its dissociation to the products is 24 kcal/mol. By use of these parameters, it was suggested[2] that 2% of the CH(O)NO would be stabilized, 50% would redissociate to the reactants, and 48% would dissociate to the products. For explanation of the smaller reactivity of vibrationally excited HCO and the modest temperature dependence of the reaction rate, the importance of the lower activation barrier to dissociation to the products compared with that to redissociation to the reactants was pointed out.[2] At the various ab initio levels, the TS1 for the CH(O)NO decomposition to HNO + CO is about 8−20 kcal/mol less stable than the reactants. Thus, it is safe to say that the dissociative reaction path through TS1 has a higher barrier than the corresponding reverse dissociation of CH(O)NO → HCO + NO, and the reverse reaction will be favored over the decomposition. This implies that the percent stabilization, redissociation, and dissociation of CH(O)NO as predicted by LM[2] would be markedly different. To explain the unusual features of the reaction, it is necessary to look for the other channels, with or without the formation of CH(O)NO, for which the activation energy is smaller than the endothermicity for the redissociation to the reactants.

III.2. Reactions of FCO + NO and ClCO + NO. The stationary structures determined at the UMP2/6-31+G(d) and B3LYP/6-311G(d) levels on the reaction paths for FCO + NO and ClCO + NO reactions are displayed in Figures 5 and 6. The structures obtained using these methods reasonably agree with each other.

We first describe the MP2 level structures and energetics**.** The energy-minimum structures of the intermediate complex CF(O)NO are a planar one with oxygens being anti around the C−N bond and a nonplanar one. The planar structure with syn oxygens has one imaginary frequency similar to the case of CH-(O)NO. The nonplanar structure is more stable than the planar anti structure by 0.3 kcal/mol, whereas the syn structure is less stable by merely 0.1 kcal/mol. For all the structures of CF-(O)NO, the harmonic frequency for the rotation of the N−O bond around the C−N bond is less than 50 cm^{-1}, implying almost free rotation. The CF(O)NO formation (step b) is an exothermic and barrierless reaction with the reaction energy of about −30 kcal/mol. The dissociation channel (step d) passes through a TS (TS1 in Figure 5 and Table 2A) in which the migrating fluorine is shared by both the carbon and nitrogen. The barrier to this process is 33.52 and 37.72 kcal/mol at the PMP2//UMP2 and QCISD(T)// UMP2 levels, respectively. The overall exothermicity of FCO + NO → FNO + CO is found to be −30.91 and −31.87 kcal/mol at the PMP2//UMP2 and QCISD(T)//UMP2 levels, respectively.

At the B3LYP/6-311G(d) level, we have considered only the anti planar structure of CF(O)NO through which all the reaction channels pass at the MP2 level. Similar to the MP2 results, this intermediate exhibits the low-frequency vibration of 80 cm^{-1}. The formation of CF(O)NO from FCO + NO is −27.20 kcal/mol exothermic without a barrier. The B3LYP binding energy is underestimated compared with the results mentioned above and is not improved by the CCSD(T)//B3LYP calculations, a trend that is similar to the results of CH(O)NO. Note that, as often pointed out, the DFT method gives smaller spin contaminations than the MO method,[12] although the structures are similar (cf. the smaller $\langle S^2 \rangle$ values in Table 2). There is a substantial difference in the overall energy of the reaction calculated with the MP2 and B3LYP structures (cf. Table 2).

With the B3LYP structures, the exothermicity is found to be underestimated (−21 kcal/mol vs −31 to −36 kcal/mol) and is not improved by the CCSD(T)//B3LYP calculations. On the other hand, the difference in the barrier to the dissociation of CF(O)NO to FNO + CO (34.07 kcal/mol) by the B3LYP method is only 4−7 kcal/mol lower than that by the QCISD-(T)//MP2 and CCSD(T)//B3LYP methods.

Higher level energy calculations for these structures (except TS1 at the PMP4//UMP2) produce qualitatively, but not quantitatively, similar energy profiles. The activation energy for the dissociative channel, CF(O)NO → FNO + CO, is larger than the endothermicity for the reverse reaction of CF(O)NO → FCO + NO. Although this trend is similar to that in the reaction of HCO + NO, the activation energy for CF(O)NO → FNO + CO (41.37 kcal/mol at the CCSD(T)//B3LYP level) is higher than that for CH(O)NO → HNO + CO (36.09 kcal/mol at the same level). This clearly supports the experimental observation that CF(O)NO is stabilized because of the higher dissociation barrier, and the reaction is pressure-dependent.[5]

All the structures of CCl(O)NO have small frequencies for the C−N bond rotation at the MP2 level. The anti planar conformer is the lowest in energy, and the syn planar isomer is the TS for the internal rotation. At the B3LYP level, only the anti planar structure has been determined**.** The energy of reaction of ClCO + NO → CCl(O)NO at the MP2/6-31+G(d) and B3LYP/6-311G(d) levels is −26.62 and −20.66 kcal/mol, respectively. Similar to the cases of CH(O)NO and CF(O)-NO, the formation energy of CCl(O)NO is underestimated at the B3LYP level compared to the QCISD(T)//MP2 estimates. This is presumably due to longer C−Cl and N−Cl distances for CCl(O)NO, ClCO, and ClNO at the B3LYP level than the corresponding MP2 ones. On the other hand, for the fluorine analogues, the C−F and N−F bond lengths at both levels are in good agreement with each other. Note that unlike X = H and F, in the case of X = Cl the restricted wave function of CCl(O)NO is stable with respect to becoming an unrestricted wave function by both the MP2 and B3LYP methods (cf. Table 3). This means that, when X = Cl, the electronic structure of CCl(O)NO has a larger character of the closed-shell systems. Thus, the dependence of relative energies on the methods is small, as long as the structure used is the same.

The barrier to the dissociative channel from CCl(O)NO is 21.49 and 14.56 kcal/mol at the PMP2//UMP2 and B3LYP//B3LYP levels, respectively. This is smaller than the endothermicity for CCl(O)NO → ClCO + NO. This implies that the dissociation of CCl(O)NO into the products ClNO + CO is more favorable or competitive compared with the redissociation to the reactants. This feature is quite different from the reactions of FCO and HCO and thus will enable the faster dissociation of CCl(O)NO to ClNO + CO. A similar trend is shown by the higher level calculations as depicted in Table 3. The exceptional result is obtained by the CCSD(T)//B3LYP calculations for which TS1 is only 1.09 kcal/mol less stable than ClCO + NO. These results suggest that the dissociation channel may be more effective than or competitive with the redissociation channel.

IV. Calculation of Rate Constants

We have calculated the rate constants for the reactions XCO + NO at room temperature using geometries and vibrational frequencies obtained theoretically. For the HCO + NO reaction, the CCSD(T)//B3LYP energies have been used for evaluation of dissociation, redissociation, and isomerization rate constants. For the reactions of NO with FCO and ClCO, we calculated the rate constants using the MP2 geometries and frequencies and the QCISD(T)//MP2 energetics as well as using the B3LYP geometries and frequencies and the CCSD(T)//B3LYP energetics. The formation of CH(O)NO from the reactants passes through a TS (cf. TSM4 in Figure 1) with almost zero barrier. We have used the simple transition-state theory (TST) to determine the rate constant for this process. For FCO + NO and ClCO + NO, a distinct TS corresponding to the formation of a collisional complex does not exist. Therefore, the TS is assumed to have a C−N bond 3.5 times longer than that in the complex.[14] The rate constants for the dissociation of CX(O)-NO have been calculated and compared with the redissociation rate constants at room temperature. The high-pressure RRKM rate constants are calculated by the versatile program UNI-MOL.[13]

Since the formation of CH(O)NO from HCO + NO has a practically zero barrier passing through TSM4, the rate constant within the simple TST expressed in cm^3 $molecule^{-1}$ s^{-1} takes the form[14]

$$k_1(T) = \left(\frac{g^{\ddagger}}{g_{CHO}g_{NO}}\right)\left(\frac{h^3}{kT}\right)\left(\frac{ABCI_D}{A'B'C'I_{NO}{}^2}\right)^{1/2}\left(\frac{m^{\ddagger}}{m_1m_2}\right)^{3/2}Q_{vib}$$

with Q_{vib} being the ratio of vibrational partition functions of TSM4 and reactants. A, B, and C are the moments of inertia (g cm^2) of TSM4, A', B', and C' are the moments of inertia of HCO, I_{NO} is that of NO, and I_D is the reduced moment of inertia for the rotation around C−N bond. g_i and m_i are the corresponding electronic multiplicities and masses. The calculated rate constant at 298 K is 2.72×10^{-11} cm^3 $molecule^{-1}$ s^{-1}, which is fairly close to the experimentally obtained[2] value of $(3.4 \pm 0.4) \times 10^{-11}$ cm^3 $molecule^{-1}$ s^{-1} .

For comparing the relative importance of the dissociation and redissociation channels, we have calculated the RRKM rate constants. The high-pressure unimolecular rate constant at 298 K for the redissociation of CH(O)NO to the reactants is 4.0×10^{-4} s^{-1} or $10^{15.54}$ exp[−108.03 kJ mol^{-1}/(*RT*)], whereas the dissociation rate constant is 5.45×10^{-14} s^{-1} or $10^{13.87}$ exp[−154.7 kJ mol^{-1}/(*RT*)]. The unimolecular rate constant for the isomerization reaction is 4.63×10^{-23} s^{-1} or $10^{11.76}$ exp[−194.42 kJ mol^{-1}/(*RT*)] at 298 K. Further, it should be noted that the magnitude of the imaginary frequency of TS corresponding to the dissociation of CH(O)NO is rather small (530i cm^{-1} at the MP2 level), indicating that the tunneling correction (calculated using the Wigner form $\kappa = 1 + [h\nu^{\#}/(k_BT)]^2/24$) will not be significant for this reaction at 298 K.

For CF(O)NO, the calculations using the MP2 structures showed that the redissociation rate constant is 8.95×10^{-9} s^{-1}, and that the dissociation takes place with a rate constant of 3.24×10^{-13} s^{-1}. The rate constants for this reaction by use of the CCSD(T)//B3LYP energetics and the B3LYP frequencies and geometrical parameters are 6.16×10^{-18} s^{-1} for the dissociation of CF(O)NO and 6.75×10^{-6} s^{-1} for redissociation to the reactants. In the case of CCl(O)NO, the dissociation rate constant calculated using the MP2 structures is found to be 2.69×10^{-4} s^{-1}, which is higher than the corresponding redissociation rate constant of 3.83×10^{-6} s^{-1}. The use of B3LYP parameters results in a dissociation rate constant of 2.65×10^{-4} s^{-1}, whereas the rate for redissociation of CCl(O)NO to the reactants is 2.86×10^{-1} s^{-1}.

The foregoing results using the ab initio energies and parameters clearly indicate that the total reaction rates may be dominated by the dissociation channel in the case of CCl(O)-NO. A comparison of the dissociation and redissociation rate constants of CX(O)NO for X = H, F, and Cl shows that the

dissociation channel is competitive only for X = Cl. On the other hand, for CH(O)NO and CF(O)NO the dissociation channel does not have any significant effect on the total reaction rates. The rate constants calculated for the reaction of CH(O)NO are not consistent with the experimentally reported forward reaction efficiency,[2] suggesting again that a different mechanism could be operative.

V. Concluding Remarks

Ab initio study at the MP2 and QCISD level as well as at the B3LYP level has been carried out on possible reactions of XCO (X = H, F, Cl) with NO. We have focused mainly on the reaction path through a collisional complex CX(O)NO. For X = H, the other possible channels have also been studied. The stationary structures are determined at the MP2 and B3LYP levels followed by the energy calculations at higher levels. For X = H, the calculations reveal that the dissociation and isomerization channels of CH(O)NO have higher barriers than the redissociation to the reactants, in contrast with the experimentally proposed profile. The present ab initio energy profile and the rate constants together suggest that the path of redissociation to the reactants is much more preferred. Thus, it is necessary to look for other reaction channels that pass through a complex with an activation energy lower than the endothermicity of the redissociation to the reactants. The proposition of such channels that fit the aforesaid requirements will be a challenge to both experimentalists and theoreticians.

Although various experimental observations seem to suggest that the potential energy surfaces of the reactions of HCO with NO and O_2 should be similar, the present work brings out the striking differences between them. In the reaction of HCO with O_2, there are mainly two channels for the disappearance of the collisional complex $HCO(O_2)$: isomerization and dissociation. The dissociation is the major channel because its barrier is lower than the barriers for isomerization and redissociation.[6] This may be attributed to the fact that the dissociation from $HCO(O_2)$ passes through the four-centered TS. In the present reaction, the TS for the dissociation from CH(O)NO has a more strained three-centered structure. Similar results should be expected in the studies of the reactions of O_2 and NO with other substrates such as the recently reported[15] reactions of HCCN.

At the MP2 level, the only channel for disappearance of CH(O)NO is via its dissociation to HNO + CO. This is a rare case wherein the MP2 level PES is not consistent with the B3LYP and QCISD ones. However, a careful analysis of the isomerization channel at the B3LYP and QCISD levels shows that the isomerization product HNOCO has only a transient existence, indicating the logical consistency of the MP2 results with other methods. Although the MP2 level calculations are routinely used for prediction of the structures and energetics of reactions, the density functional methods provide a reliable and cost-effective estimates of it.

For the reactions of FCO + NO and ClCO + NO, the structures and relative energies calculated at both the MP2 and B3LYP levels are in a fair agreement with each other. The dissociation channel has a higher barrier than the redissociation of CF(O)NO at all higher level calculations, implying greater probabilities of the redissociation or stabilization of the complex. The pressure dependence of the reaction indicates that stabilization of the complex is more plausible. The dissociation channel from CCl(O)NO could be the major channel for the product formation. However, other low-barrier channels cannot be ruled out. It is felt that further detailed investigations are necessary for exploring them.

Acknowledgment. S.A.K. and N.K. thank the Ministry of Education, Culture, Sports, and Sciences of Japan (Monbusho) for a scholarship and for a Grants-in-Aid, respectively. Part of the calculations were carried out at the computer center of Institute for Molecular Science, Japan. We are grateful to the referees for suggesting several improvements.

References and Notes

(1) Shibuya, K.; Ebata, T.; Obi, K.; Tanaka, I. *J. Phys. Chem.* **1977**, *81*, 2292. Veyret, B.; Lesclaux, R. *J. Phys. Chem.* **1981**, *85*, 1918.

(2) Langford, A. O.; Moore, C. B. *J. Chem. Phys*. **1984**, *80*, 4211.

(3) Tsang, W.; Herron, J. T. *J. Phys. Chem. Ref. Data* **1991**, *20* 609.

(4) Willington, T. J.; Ellermann, T.; Neilsen, O. J.; Sehested, J. *J. Phys. Chem.* **1994**, *98*, 2346.

(5) Behr, P.; Shafranovsky, E.; Heydtmann, H. *Chem. Phys. Lett*. **1995**, *247*, 327.

(6) Hsu, C. C.; Mebel, A. M.; Lin, M. C. *J. Chem. Phys*. **1996**, *105*, 2346.

(7) Francisco, J. S.; Zhao, Y. *Chem. Phys. Lett*. **1988**, *153*, 296.

(8) Francisco, J. S.; Goldstein, A. N.; Li, Z.; Zhao, Y.; Williams, I. H. *J. Phys. Chem.* **1990**, *94*, 4791.

(9) Frisch, M. J.; Trucks, G. W.; Schlegel, H. B.; Gill, P. M. W.; Johnson, B. G.; Robb, M. A.; Cheeseman, J. R.; Keith, T.; Petersson, G. A.; Montgomery, J. A.; Raghavachari, K.; Al-Laham, M. A.; Zakrzewski, V. G.; Ortiz, J. V.; Foresman, J. B.; Peng, C. Y.; Ayala, P. Y.; Chen, W.; Wong, M. W.; Andres, J. L.; Replogle, E. S.; Gomperts, R.; Martin, R. L.; Fox, D. J.;. Binkley, J. S.; Defrees, D. J.; Baker, J.; Stewart, J. J. P.; Head-Gordon, M.; Gonzalez, C.; Pople, J. A. *Gaussian 94*, Revision B.3; Gaussian, Inc.: Pittsburgh, PA, 1995.

(10) Curtiss, L. A.; Raghavachari, K.; Pople, J. A. *J. Chem. Phys*. **1993**, *98*, 1293.

(11) Frisch, M. J.; Trucks, G. W.; Cheeseman, J. R. *Recent Developments and Applications of Modern Density Functional Theory*; Seminario, J. M., Ed.; Theoretical and Computational Chemisty 4; Elsevier: Amsterdam, 1996; p 679.

(12) Baker, J.; Scheiner, A.; Andzelm, J. *Chem. Phys. Lett*. **1994**, *216*, 380. Johnson, B. G.; Gonzales, C. A.; Gill, P. M. W.; Pople, J. A. *Chem. Phys. Lett*. **1994**, *221*, 100.

(13) Gilbert, R. G.; Smith, S. C.; Jordan, M. J. T. *UNIMOL* (program suite), 1993. See also the following. Gilbert, R. G.; Smith S. C. *Theory of Unimolecular and Recombination Reactions*; Blackwell Scientific: Oxford, 1990.

(14) Abou-Rachid, H.; Pouchan, C.; Chaillet, M. *Chem. Phys*. **1984**, *90*, 243.

(15) Adamson, J. D.; Desain, J. D.; Curl, R. F.; Glass, G. P. *J. Phys. Chem. A* **1997**, *101*, 864.